

Electronic Supplementary Information for

Catalytic Coupling of CO₂ with Epoxide by the Ionic Liquid Modified Metal Macrocycles: Insight into Mechanism and Activity Regulation from Density functional Calculations

Ping Li and Zexing Cao*

State Key Laboratory of Physical Chemistry of Solid Surfaces, Fujian Provincial Key Laboratory of Theoretical and Computational Chemistry, and College of Chemistry and Chemical Engineering, Xiamen University, Xiamen 360015, China

E-mail: zxcao@xmu.edu.cn; Fax: (+86) 592-218-3047; Tel: (+86) 592-218-6081

Table of Contents

Fig. S1 Optimized structures (bonds in Å) of species for the cycloaddition reaction of CO₂ and PO catalyzed by IL-Zn(TPP) and the Zn as the catalytic center.

Fig. S2 Predicted relative free energy profile and electronic energies (in parentheses) for the cycloaddition reaction of CO₂ and PO catalyzed by IL-Zn(TPP) and the imidazole as the catalytic center.

Fig. S3 Optimized structures (bonds in Å) of species for the cycloaddition reaction of CO₂ and PO catalyzed by IL-Zn(TPP) and the imidazole as the catalytic center.

Fig. S4 Optimized structures (bonds in Å) of species for the cycloaddition reaction of CO₂ and PO catalyzed by IL-Zn(TPP) and the COOH group as the catalytic center.

Fig. S5 Predicted relative free energy profile and electronic energies (in parentheses) for the cycloaddition reaction of CO₂ and PO catalyzed by the metalloporphyrin moiety of COOH-IL-Zn(TPP).

Fig. S6 Optimized structures (bonds in Å) of species for the catalytic cycloaddition reaction of CO₂ and PO by COOH-IL-Zn(TPP).

Fig. S7 Predicted relative free energy profile and electronic energies (in parentheses) for the catalytic cycloaddition reaction of CO₂ and PO by COOH-IL-Mg(TPP).

Fig. S8 Optimized structures (bonds in Å) of species for the catalytic cycloaddition reaction of CO₂ and PO by COOH-IL-Mg(TPP).

Fig. S9 Optimized structures (bonds in Å) of species involved in the catalytic cycloaddition reaction of CO₂ and PO by the IL moiety of IL-Al(Cor).

Fig. S10 Optimized structures (bonds in Å) of species for the catalytic cycloaddition reaction of CO₂ and PO by COOH- IL-Al(Cor).

Fig. S11 Predicted relative free energy profile and electronic energies (in parentheses) for the catalytic cycloaddition reaction of CO₂ and PO by the IL moiety of COOH-IL-Al(Cor).

Fig. S12 Optimized structures (bonds in Å) of species for the catalytic cycloaddition reaction of CO₂ and PO by the IL moiety of OH- IL-Al(Cor).

Fig. S13 Predicted relative free energy profile and electronic energies (in parentheses) for the catalytic cycloaddition reaction of CO₂ and PO by the IL moiety of OH-IL-Al(Cor).

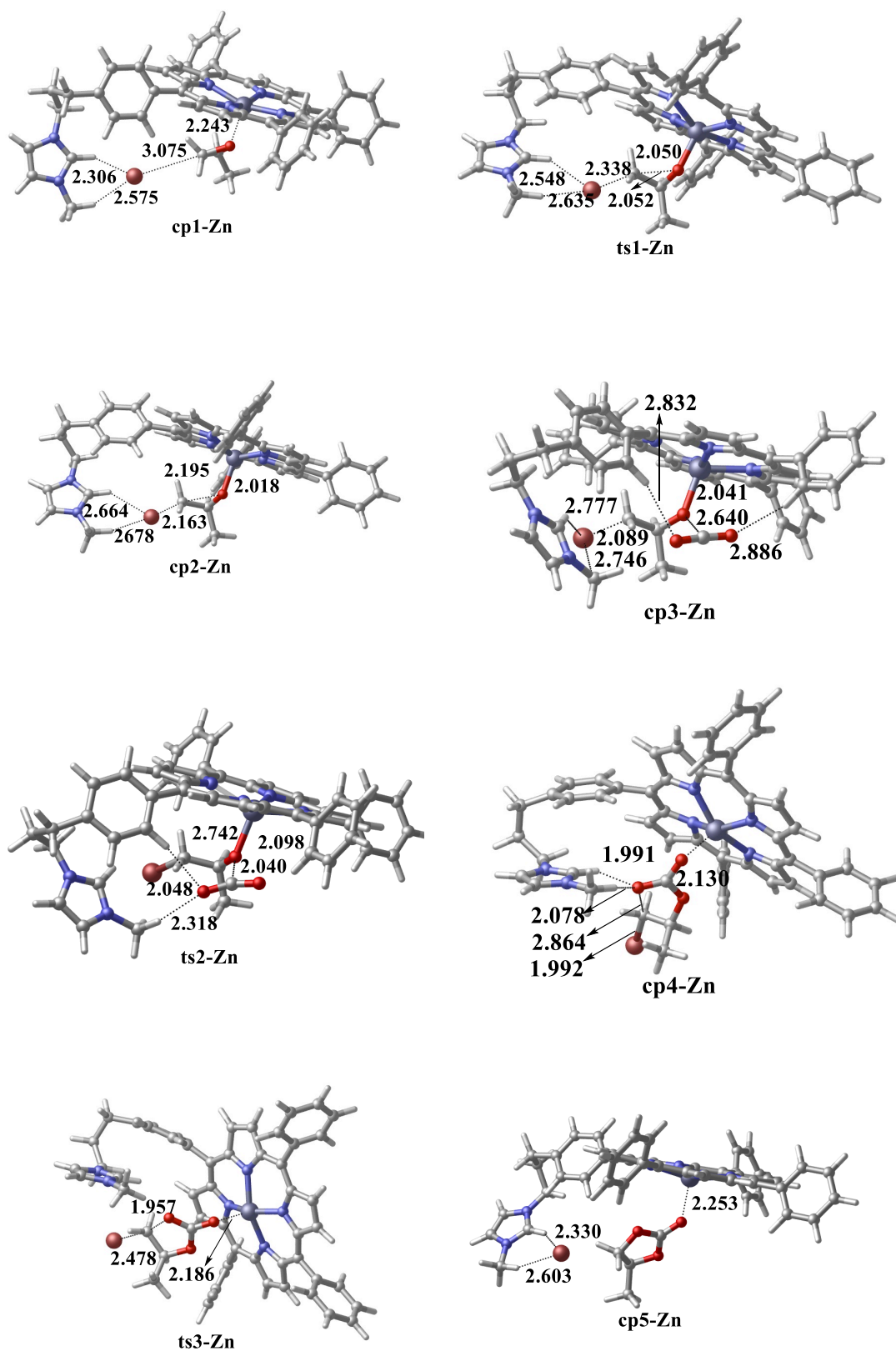


Fig. S1 Optimized structures (bonds in Å) of species for the cycloaddition reaction of CO₂ and PO catalyzed by IL-Zn(TPP) and the Zn as the catalytic center.

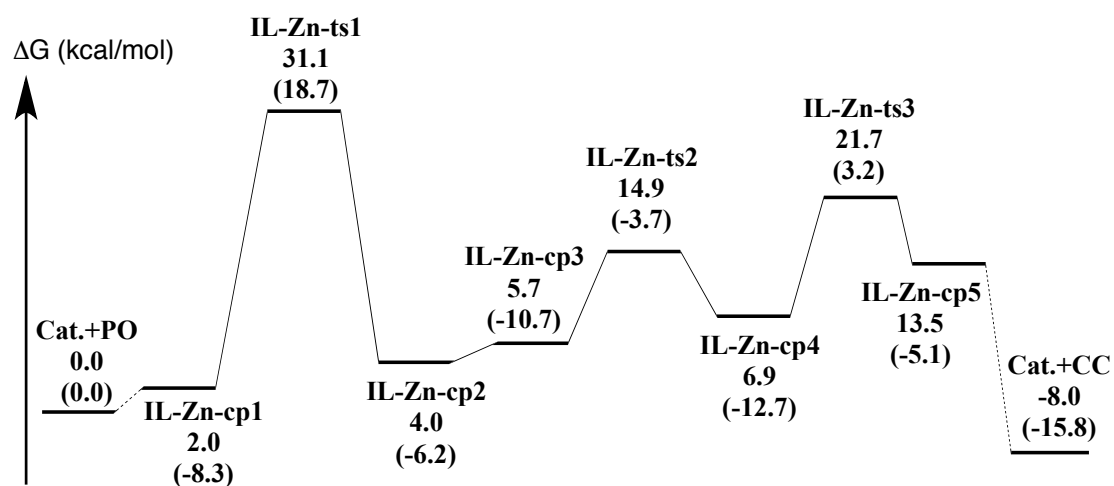
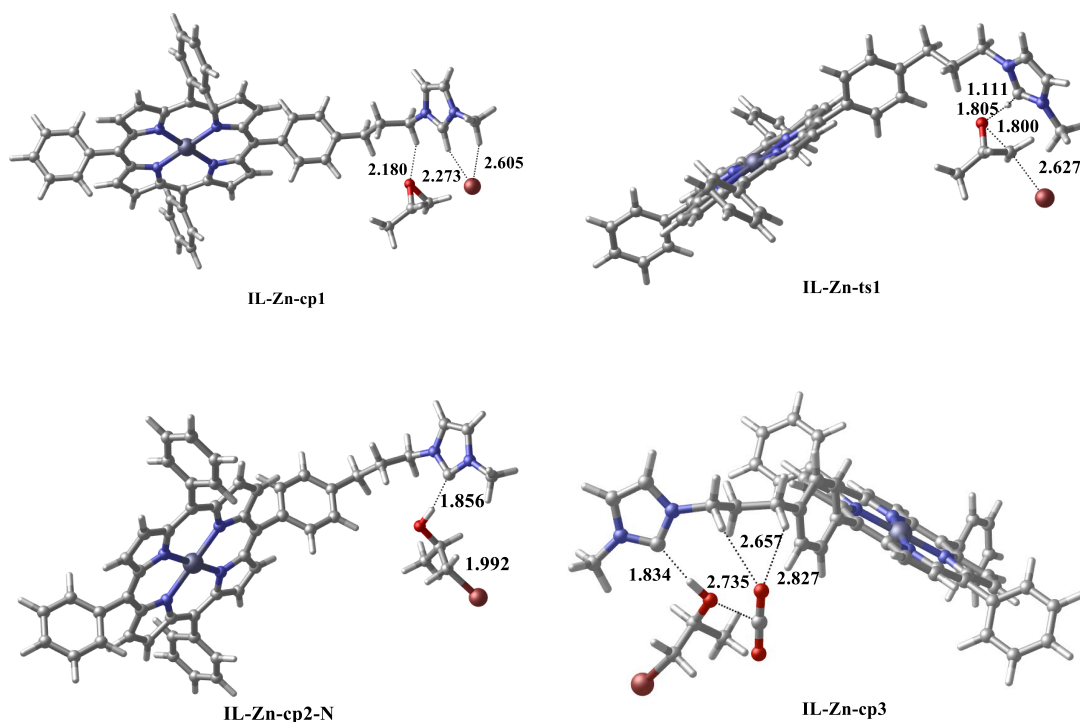


Fig. S2 Predicted relative free energy profile and electronic energies (in parentheses) for the cycloaddition reaction of CO₂ and PO catalyzed by IL-Zn(TPP) and the imidazole as the catalytic center.



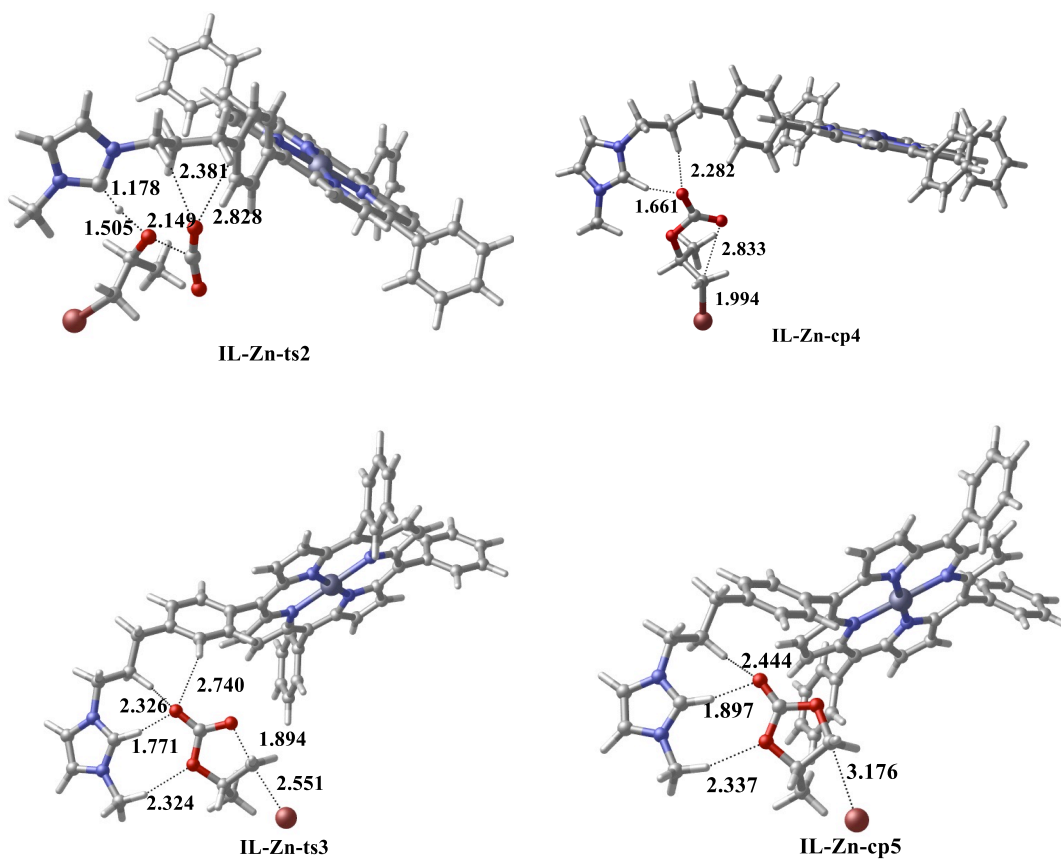
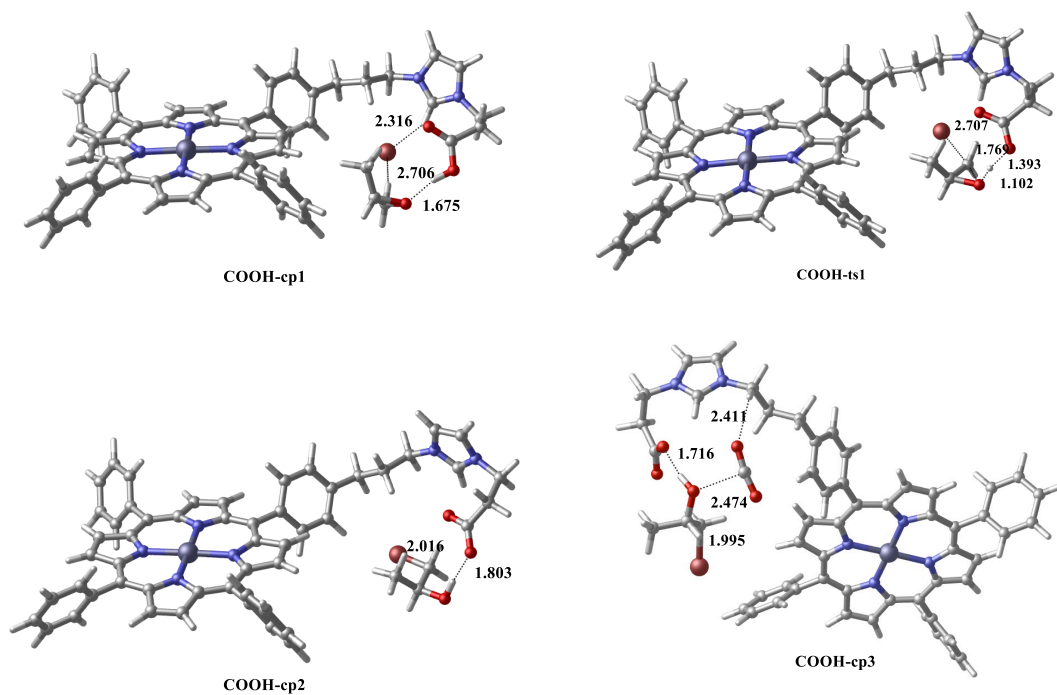


Fig. S3 Optimized structures (bonds in Å) of species for the cycloaddition reaction of CO₂ and PO catalyzed by IL-Zn(TPP) and the imidazole as the catalytic center.



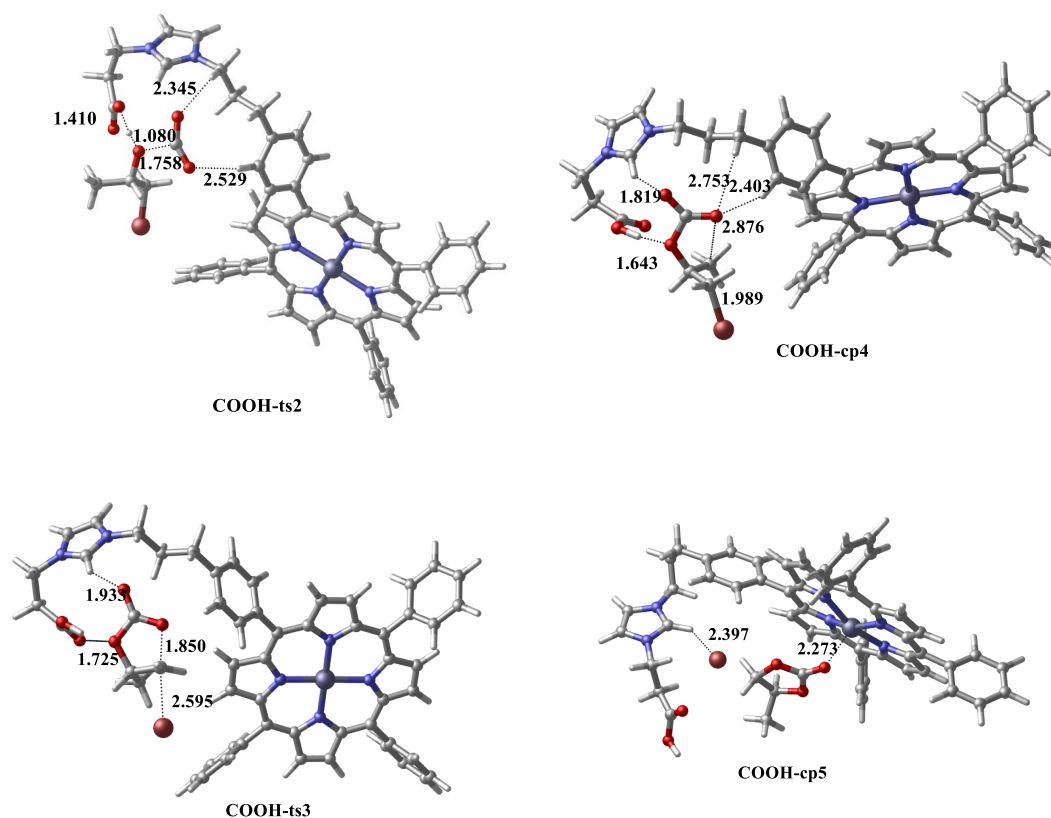


Fig. S4 Optimized structures (bonds in Å) of species for the cycloaddition reaction of CO₂ and PO catalyzed by IL-Zn(TPP) and the COOH group as the catalytic center.

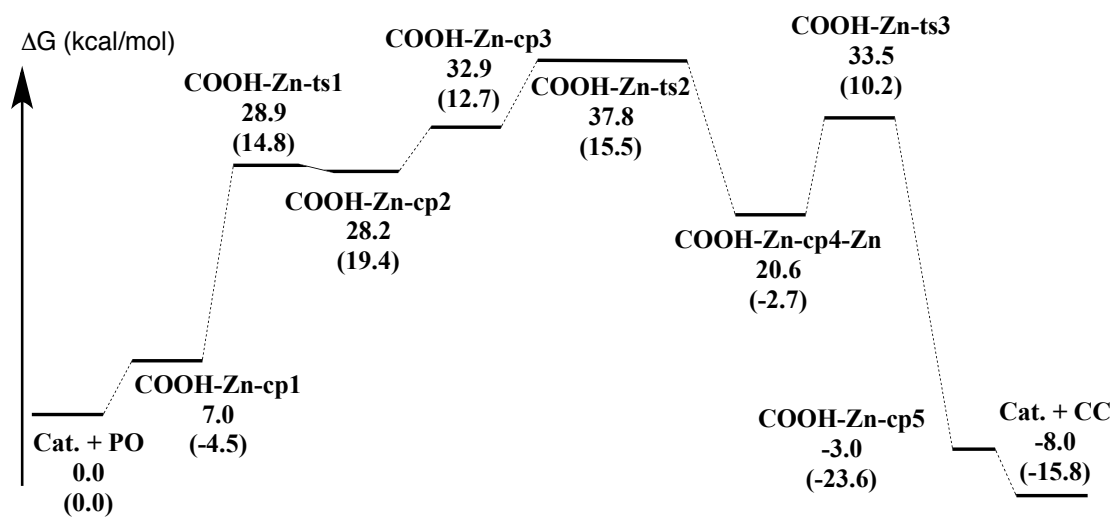


Fig. S5 Predicted relative free energy profile and electronic energies (in parentheses) for the cycloaddition reaction of CO₂ and PO catalyzed by the metalloporphyrin moiety of COOH-IL-Zn(TPP).

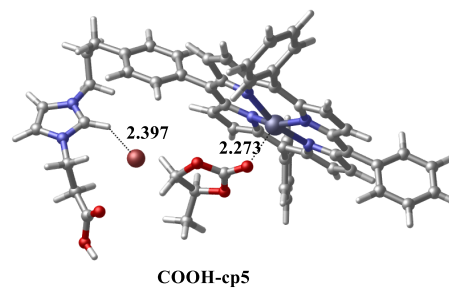
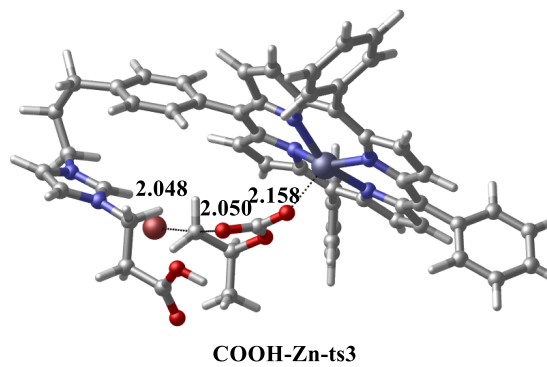
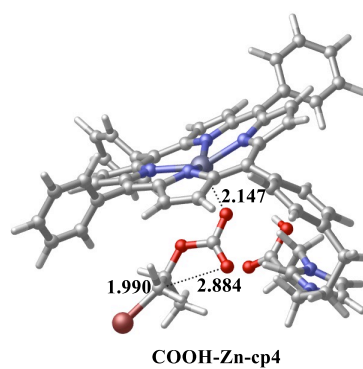
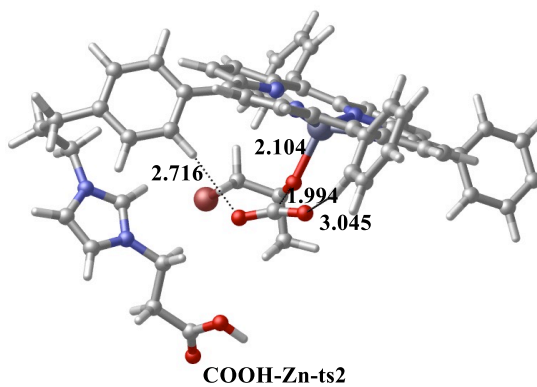
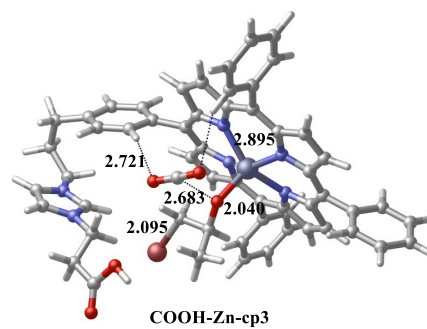
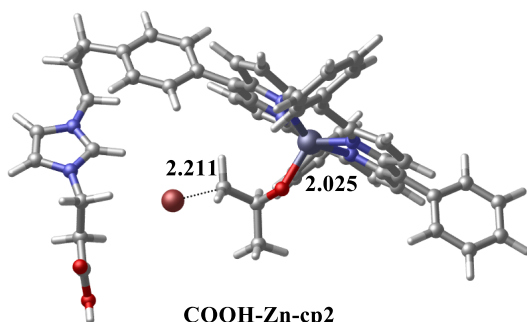
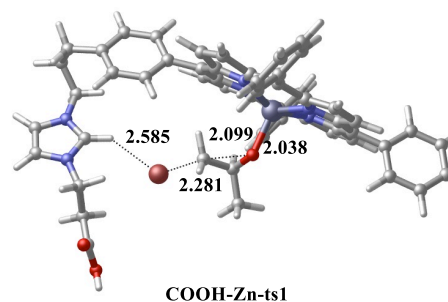
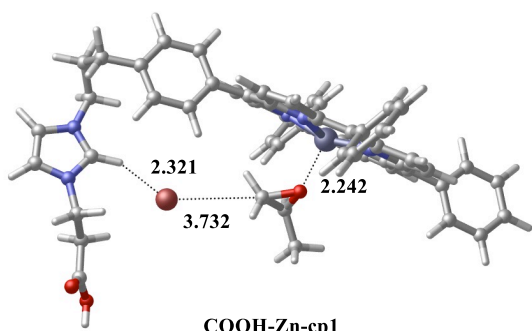


Fig. S6 Optimized structures (bonds in Å) of species for the catalytic cycloaddition reaction of CO₂ and PO by COOH-IL-Zn(TPP).

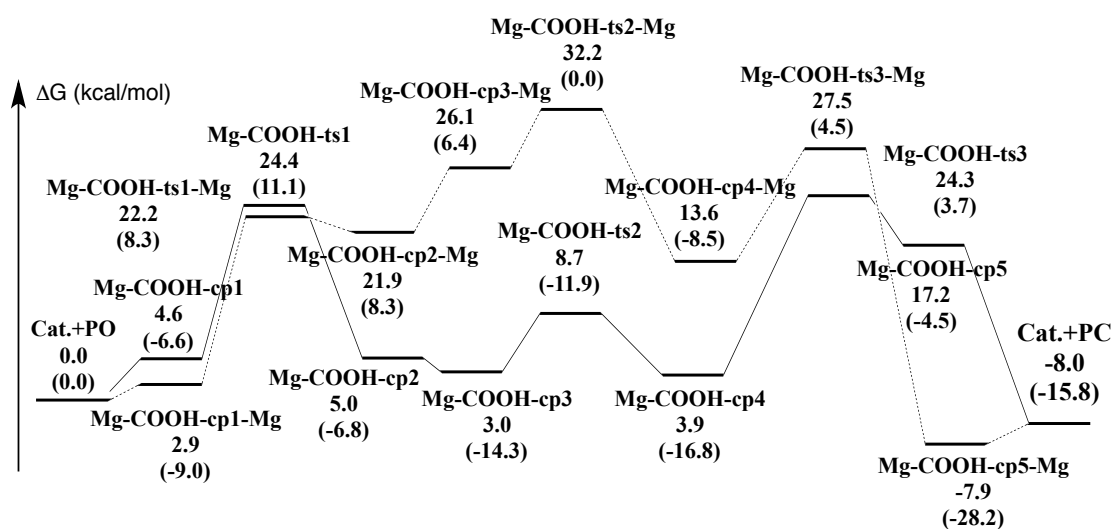
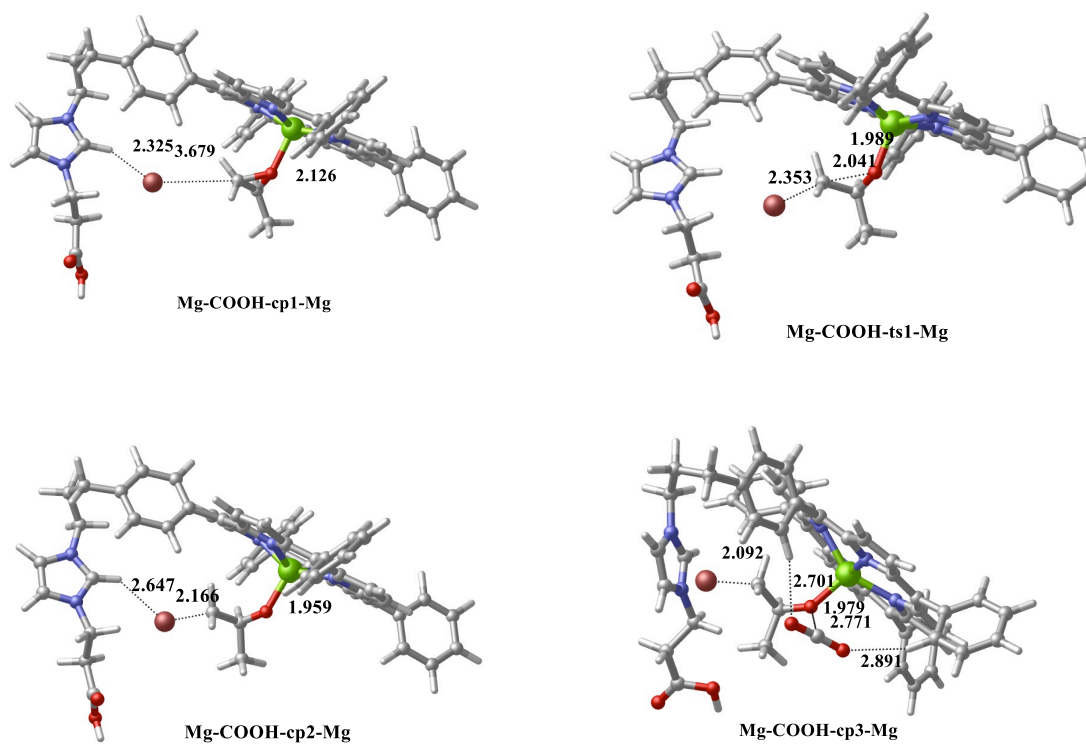
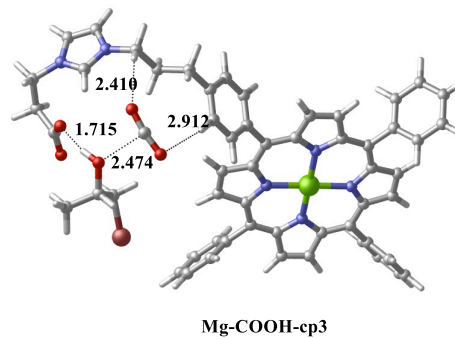
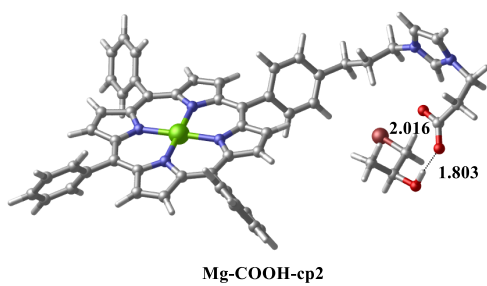
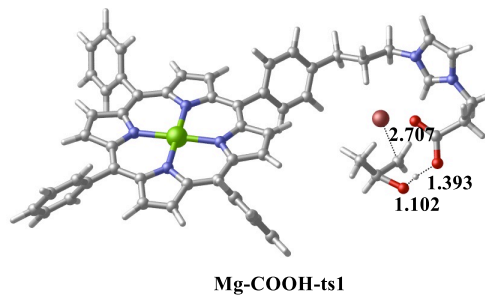
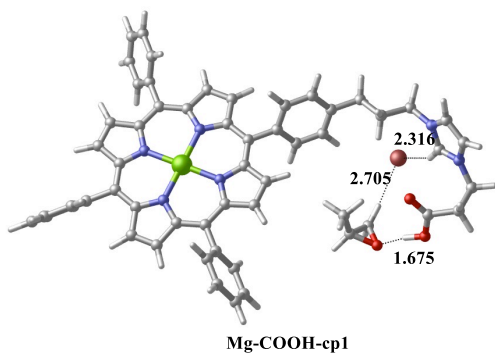
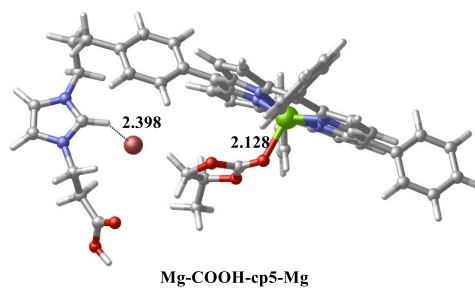
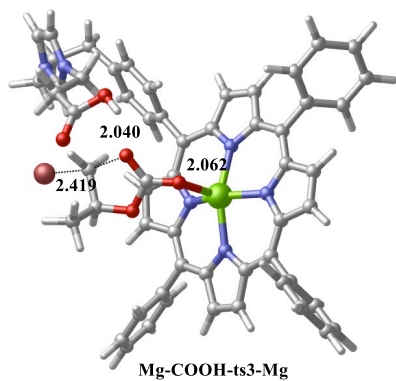
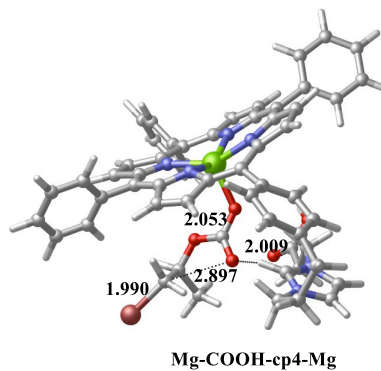
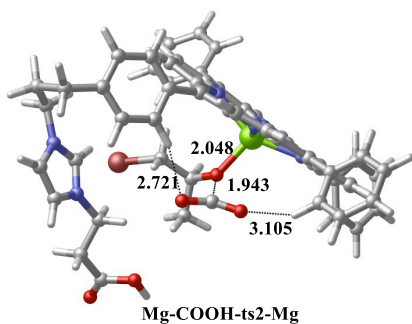


Fig. S7 Predicted relative free energy profile and electronic energies (in parentheses) for the catalytic cycloaddition reaction of CO₂ and PO by COOH-IL-Mg(TPP).





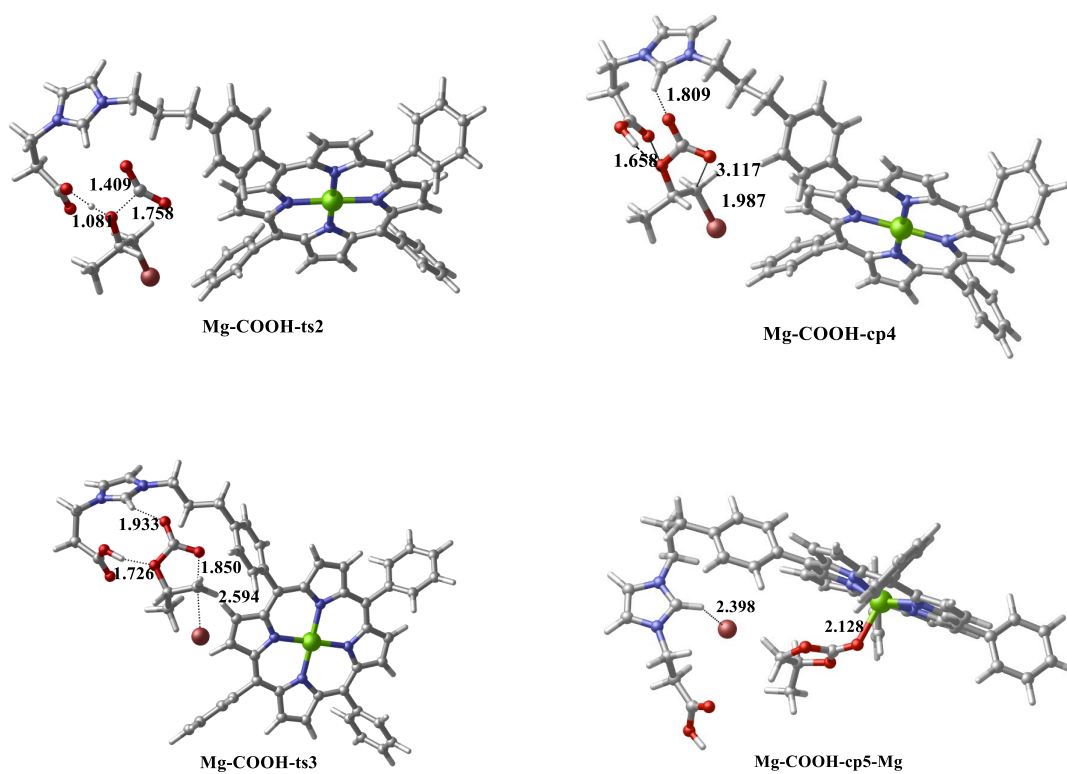
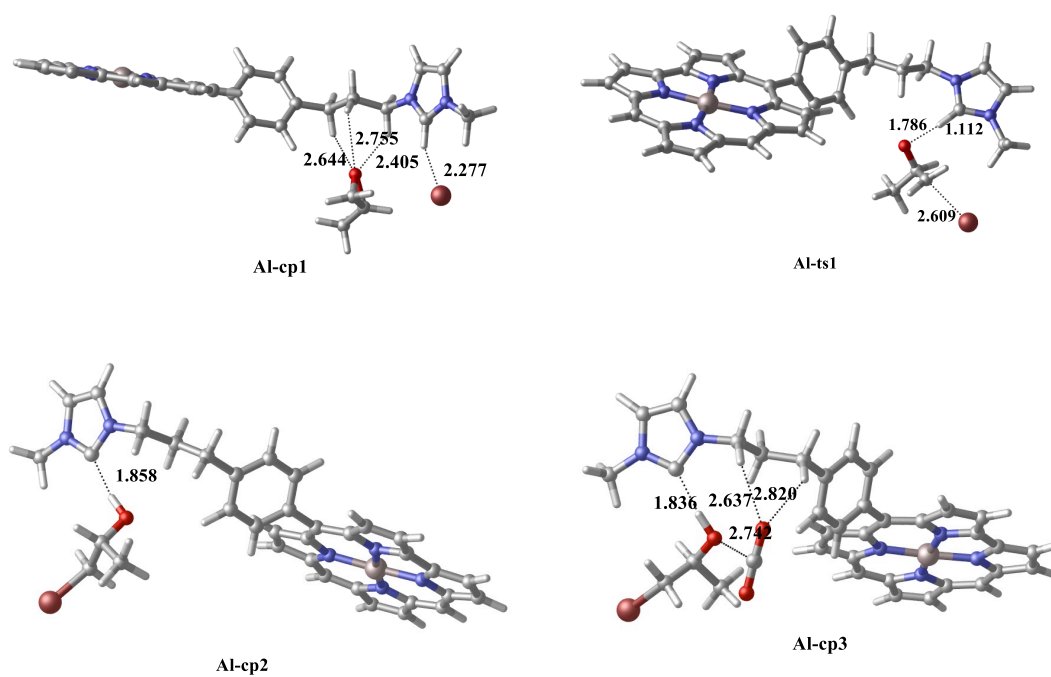


Fig. S8 Optimized structures (bonds in Å) of species for the catalytic cycloaddition reaction of CO₂ and PO by COOH-IL-Mg(TPP).



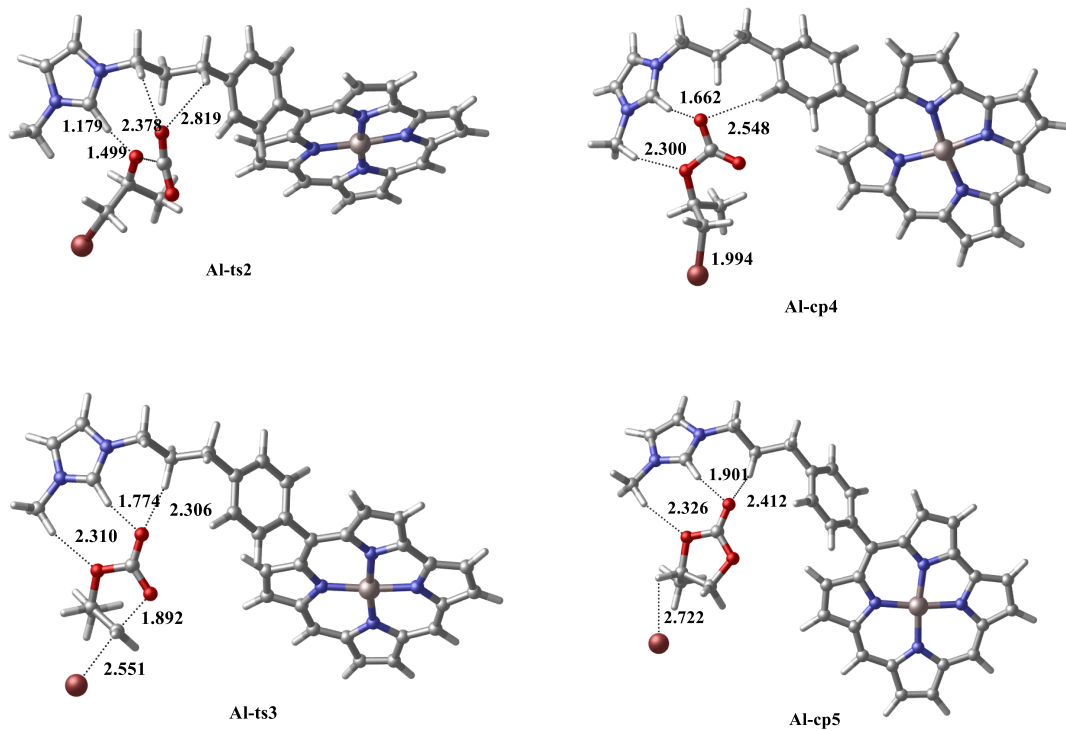
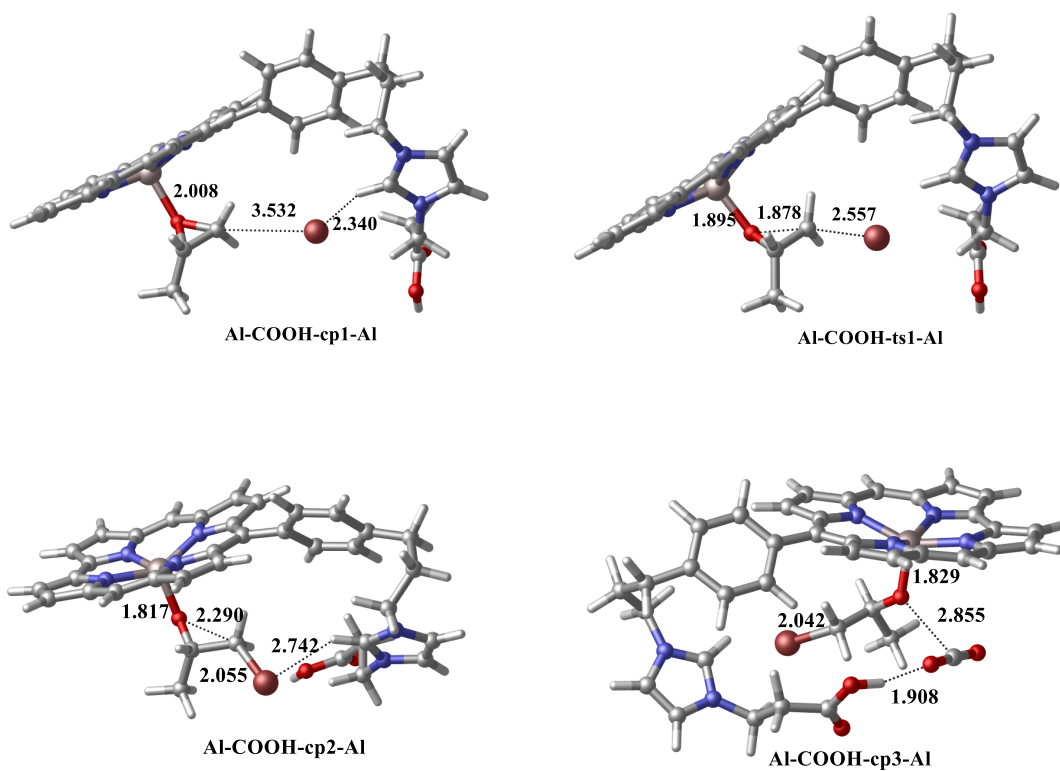
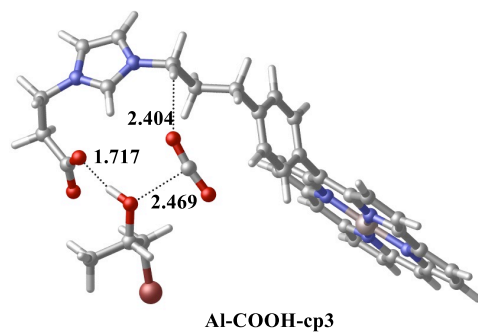
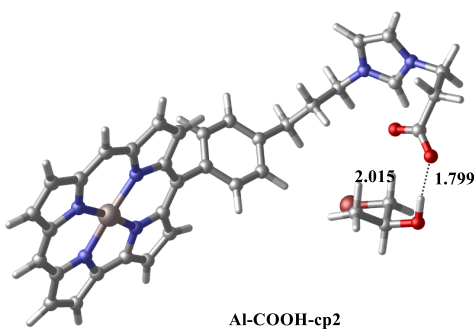
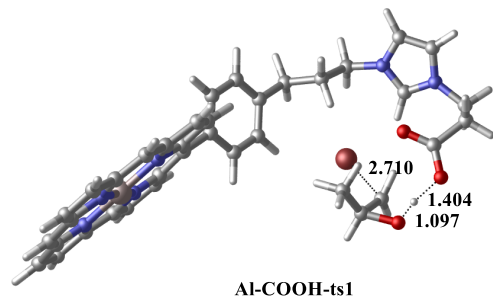
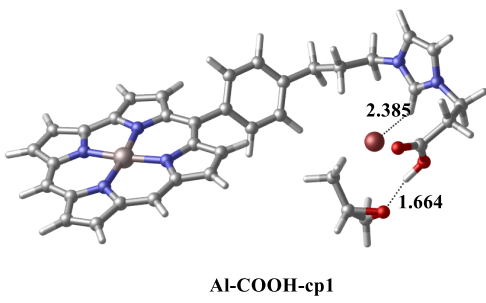
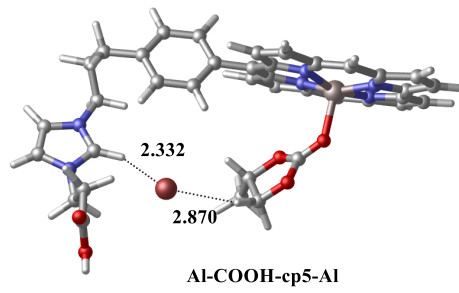
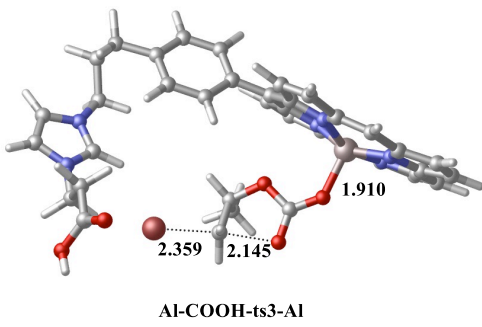
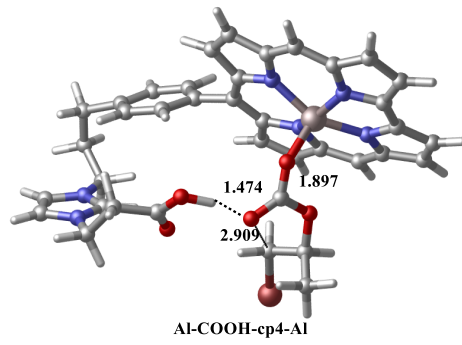
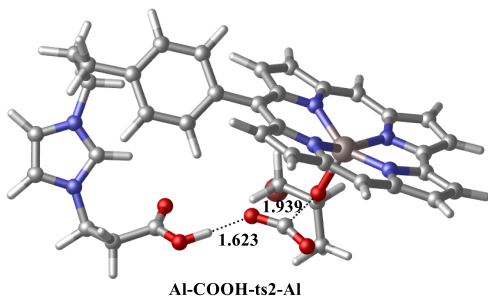


Fig. S9 Optimized structures (bonds in Å) of species involved in the catalytic cycloaddition reaction of CO₂ and PO by the IL moiety of IL-Al(Cor).





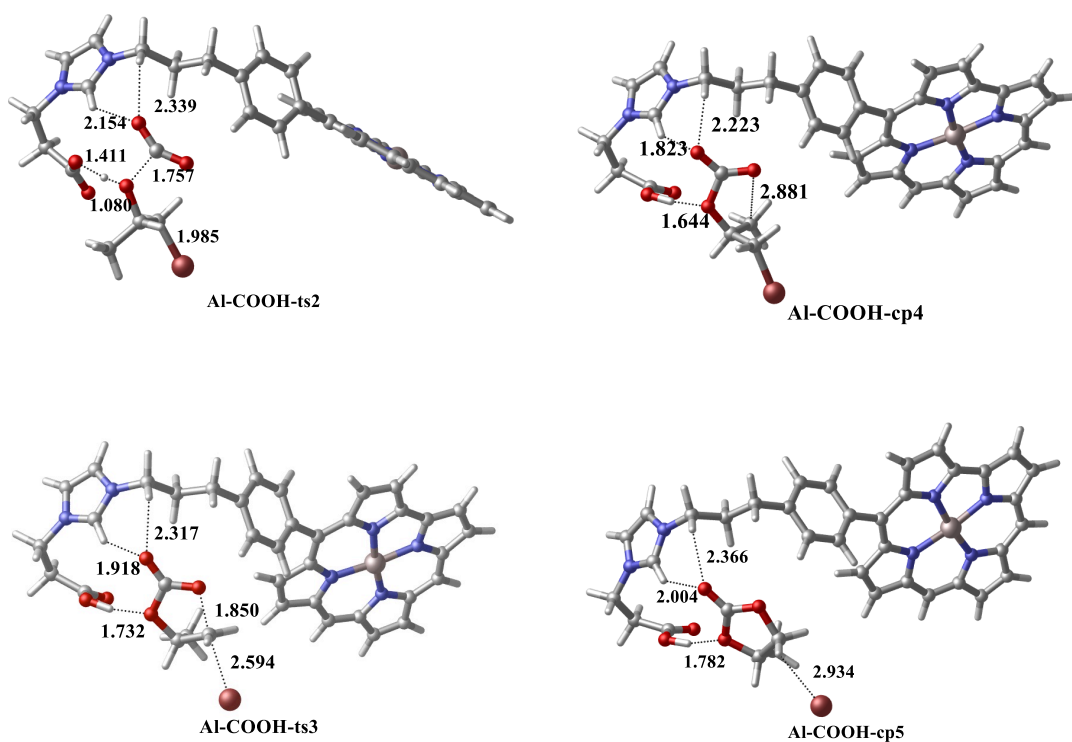


Fig. S10 Optimized structures (bonds in Å) of species for the catalytic cycloaddition reaction of CO₂ and PO by COOH-IL-Al(Cor).

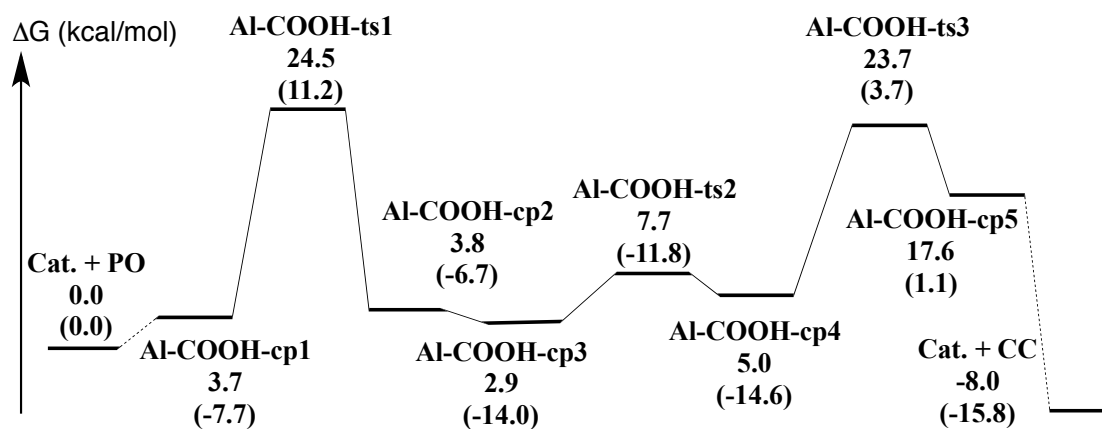


Fig. S11 Predicted relative free energy profile and electronic energies (in parentheses) for the catalytic cycloaddition reaction of CO₂ and PO by the IL moiety of COOH-IL-Al(Cor).

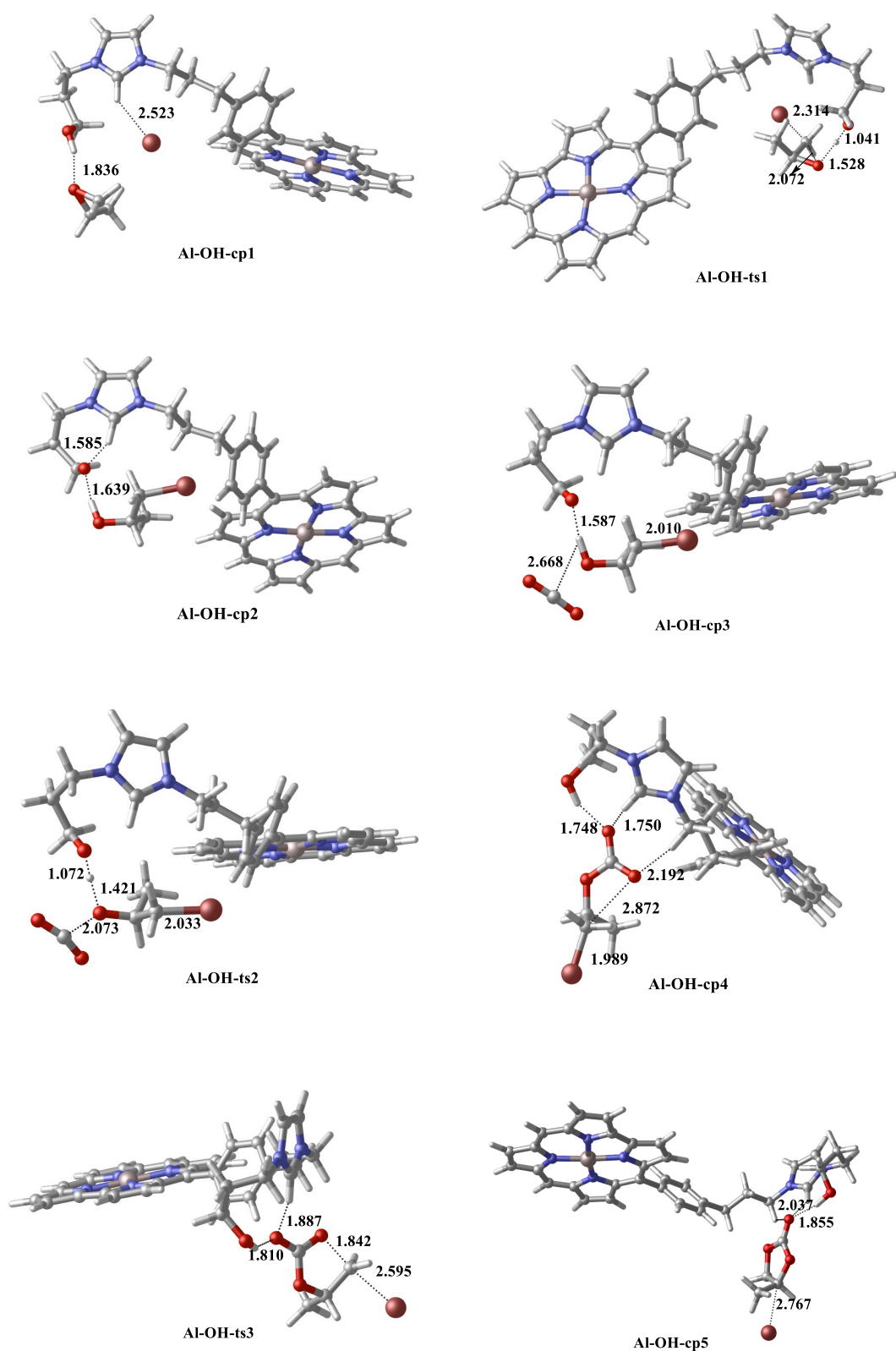


Fig. S12 Optimized structures (bonds in Å) of species for the catalytic cycloaddition reaction of CO₂ and PO by the IL moiety of OH-IL-Al(Cor).

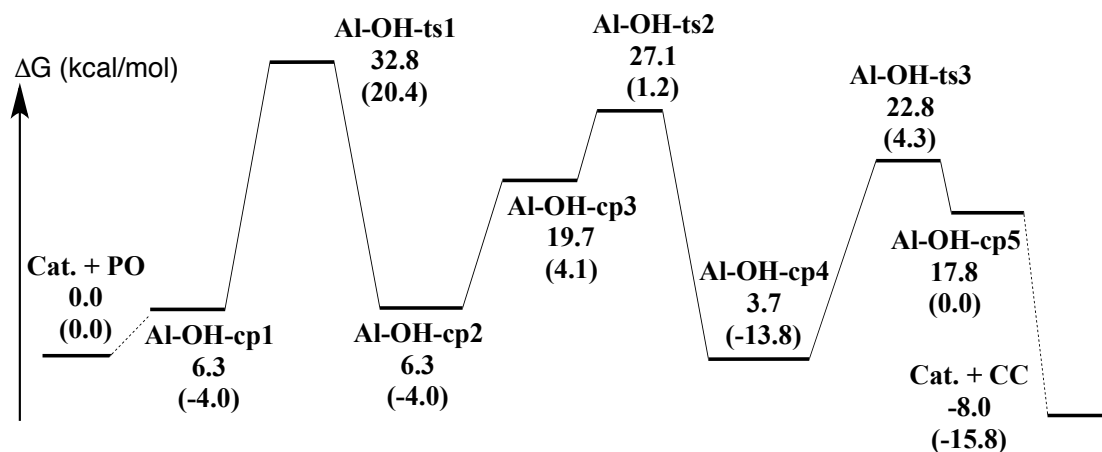


Fig. S13 Predicted relative free energy profile and electronic energies (in parentheses) for the catalytic cycloaddition reaction of CO₂ and PO by the IL moiety of OH-IL-Al(Cor).